Journal of Alloys and Compounds 509 (2011) 1734–1738

Contents lists available at ScienceDirect

Journal of Alloys and Compounds

journal homepage: www.elsevier.com/locate/jallcom

Effects of compaction pressure on the electrochemical properties of Mm0.3Ml0.7Ni3.55Co0.75Mn0.4Al0.3 metal hydride electrodes

Xiao Tian[a,b,*], Xiang-dong Liu[a], Fan Ma[a], Yali Nie[a], Jin Xu[c]

[a] School of Materials Science and Engineering, Inner Mongolia University of Technology, Huhhot 010051, PR China
[b] School of Physics and Electronic Information, Inner Mongolia Normal University, Huhhot 010022, PR China
[c] Zhanjiang Radio and TV University, Zhanjiang 524003, PR China

ARTICLE INFO

Article history:
Received 19 April 2010
Received in revised form
30 September 2010
Accepted 7 October 2010
Available online 15 October 2010

Keywords:
Hydrogen storage alloy
Ni/MH battery
Compaction pressure
Electrochemical property

ABSTRACT

In this work, the negative electrodes of the nickel–metal hydride rechargeable batteries were prepared at different compaction pressures. The maximum discharge capacities and cycle stabilities of the electrodes were measured by means of electrochemical method. The crystal structures and surface morphologies of the alloys were intensively studied by X-ray diffraction (XRD) and scanning electron microscopy (SEM) combined with energy-dispersive spectrometry (EDS), respectively. Based on these observations, the effects of compaction pressure on the electrochemical properties of the electrodes were systematically investigated. The results showed that the electrode prepared at a compaction pressure of 25 MPa exhibited the best discharge capacity and better cycle stability.

1. Introduction

Although nickel–metal hydride (Ni/MH) rechargeable batteries show numerous advantages when compared with conventional batteries, improvements to Ni/MH batteries are still necessary in order to meet increasing market demands. Such improvements include higher discharge capacity, longer cycle life, better kinetic behavior and lower cost. The metal hydride electrode plays a very important role in allowing these improvements as the active negative electrode in Ni/MH batteries.

It is well known that the electrochemical activity of the metal hydride electrode is determined not only by hydrogen storage alloy but also by the preparation technology of the electrode [1–3]. The hydrogen storage alloys used as the main negative materials of Ni/MH batteries have been extensively studied in recent decades, and several series of hydrogen storage alloys have been developed, including AB_5-type alloys, AB_2-type alloys, Mg-based alloys and AB_3-type alloys, etc. [4–19]. On the other hand, the parameters of the metal hydride electrode preparation, such as the particle sizes of the hydrogen storage alloys, conductive materials, the mass ratios of conductive materials to hydrogen storage alloys, the compaction pressure and the pressure-holding time during electrode preparation, are also of great importance to improve electrochemical properties and reduce the total weight and the cost of the negative electrodes. In recent years, some researches have concentrated on the effects of particle size of the hydrogen storage alloy, conductive materials and the mass ratios of conductive materials to hydrogen storage alloys on the electrochemical properties of electrodes and great achievements have been made [20–23]. However, it is found in our research work that compaction pressure has a great effect on the electrochemical properties of metal hydride electrodes during long-term electrochemical measurement process. Though the effects of compaction pressure on the performances of the electrode have been reported previously [24,25], the investigations mainly focused on the effects of compaction pressure on the discharge capacities and rate capabilities of the electrode and the mechanism of the effects has not been discussed yet.

In order to obtain the correct parameters of hydrogen storage electrode preparation, $Mm_{0.3}Ml_{0.7}Ni_{3.55}Co_{0.75}Mn_{0.4}Al_{0.3}$ metal hydride electrodes were prepared at different compaction pressures, and their electrochemical properties are systematically investigated. The mechanism of the effects of compaction pressure on the electrochemical properties of electrodes was also discussed.

2. Experimental

The $Mm_{0.3}Ml_{0.7}Ni_{3.55}Co_{0.75}Mn_{0.4}Al_{0.3}$ alloy was melted in induction furnace under argon atmosphere. The Ce-rich misch metal (Mm) consisted of 26.4 wt.% La, 53.1 wt.% Ce, 5.2 wt.% Pr, and 15.3 wt.% Nd. The La-rich misch metal (Ml) con-

* Corresponding author at: School of Physics and Electronic Information, Inner Mongolia Normal University, Zhaowuda Road 81#, Huhhot 010022, PR China. Tel.: +86 013154809983.
E-mail addresses: nsdtx@126.com, nsdtx@imnu.edu.cn (X. Tian).

0925-8388/$ – see front matter © 2010 Elsevier B.V. All rights reserved.
doi:10.1016/j.jallcom.2010.10.025

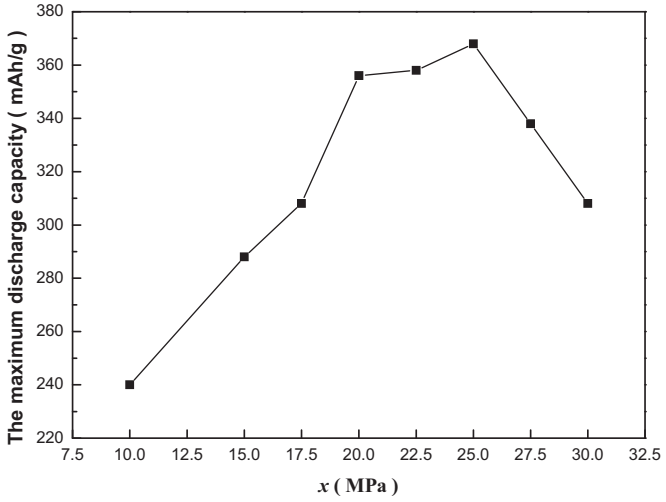

Fig. 1. The relationship between the maximum discharge capacity of the alloy electrode and compaction pressure.

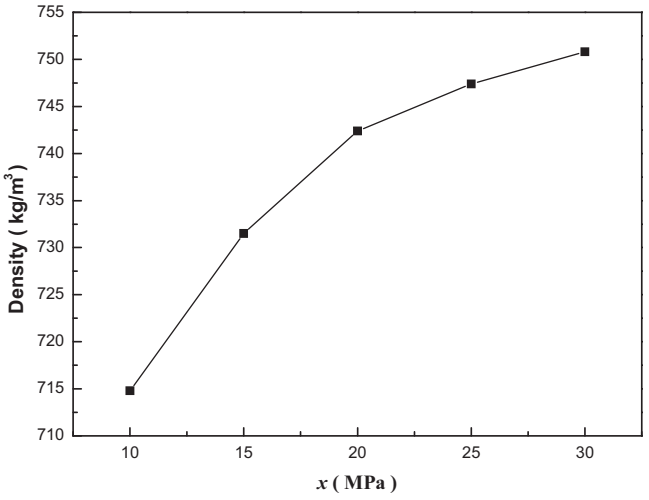

Fig. 2. Variation of the density of electrodes with the compaction pressures.

tained 62.9 wt.% La, 26.1 wt.% Ce, 2.7 wt.% Pr, and 8.3 wt.% Nd. The purity of all the component metals (Ni, Co, Mn, Al) was at least 99.8 wt.%. Part of the alloys were mechanically crushed and ground into powders with a dimension of 250-mesh for electrochemical measurements.

For the electrodes preparation, all test alloy electrodes were first prepared by thoroughly mixing 0.25 g alloy powders with 0.75 g carbonyl nickel powders and cold pressing the mixture at a compaction pressure of x (x = 10, 15, 17.5, 20, 22.5, 25, 27.5 and 30 MPa) for 15 min into round electrode pellets of 15 mm in diameter. Then the electrode pellets were enwrapped with foam nickel. A nickel lead wire was attached to the foam nickel sheet by spot welding. Finally, the electrodes were immersed in 6 M KOH solution for 24 h to ensure complete wetting before the electrochemical measurement.

The experimental electrodes were tested at ambient temperature in a tri-electrode, a working electrode (metal hydride electrode), a counter electrode ($NiOOH/Ni(OH)_2$) with a large capacity and a reference electrode (Hg/HgO), open cell. The electrolyte used was a 6 M KOH solution. The electrochemical properties were measured using a Battery Test System. Each electrode was charged at 100 mA/g for 5 h followed by 5 min rest and then discharged at 60 mA/g to the cut-off potential of −0.600 V vs. the Hg/HgO reference electrode. The maximum discharge capacity was noted as C_{max}. In the cycle stability measurement, after being completely activated, each electrode was charged at 300 mA/g for 1.5 h followed by 20 min rest and then discharged at 300 mA/g to the cut-off potential of −0.600 V vs. the Hg/HgO reference electrode. In order to confirm the change of the discharge capacity of the electrode, after successive periods of 50 cycles, each electrode was charged at 100 mA/g for 5 h followed by 5 min rest and then discharged at 60 mA/g to the cut-off potential of −0.600 V vs. the Hg/HgO reference electrode.

The crystal structure of the alloy was determined by X-ray powder diffraction (XRD) using CuK_α radiation. The surface morphology of the alloy was examined using scanning electron microscopy (SEM) combined with energy-dispersive spectrometry (EDS).

3. Results and discussion

Fig. 1 shows the relationship between the maximum discharge capacity of the alloy electrode and compaction pressure. It can be seen that, when x increases from 10 MPa to 25 MPa, the maximum discharge capacity of the electrode firstly increases from 240 mAh/g to 368 mAh/g, and then decreases to 308 mAh/g with x further increasing to 30 MPa. This result indicates that the compaction pressure has significant effect on the maximum discharge capacity of the electrode.

In general, the maximum discharge capacity of the electrode is intimately related to the electrochemical reactions of the hydrogen storage alloy during the charging/discharging cycle process. The electrochemical reactions of the hydrogen storage alloys are closely related to the following two aspects: (1) the surface characteristics of the alloy particles which control the charge-transfer reaction rate on the alloy surface. These include the thickness of oxide layer on the alloy particles surface, the composition of the alloy particles surface, the gap between the surfaces of the alloy particles, and so on. (2) The structure characteristics of the hydrogen storage alloy itself, which control the hydrogen diffusion rate in the bulk of the alloys. These include lattice parameter, cell volume, interstitial size, diffusion coefficient of hydrogen atoms in alloy, and so on [21].

In this work, it is difficult that new compounds are generated during electrode preparation process due to conductive materials powders just mechanically mixing with the hydrogen storage alloys powders and then the mixture being cold pressed for shorter time. The effects of compaction pressure on the maximum discharge capacity of the electrodes should be attributed to the surface characteristics of the alloy particles, which control the charge-transfer reaction rate on the alloy surface. For the smaller compaction pressure, the contacts between the alloy particles or the alloy particles and the conductive materials are not tight. The oxide layers form easily on the surface of the alloy particles. The oxide layers interfere with close contact of the fresh surfaces of alloy particles with the alkaline electrolyte during the electrochemical reactions. As a result, the charge-transfer reaction rate at the surface of the alloy particles is restrained and no more hydrogen atoms can enter into the crystal lattice. This leads directly to the lowest maximum discharge capacity of the electrode prepared

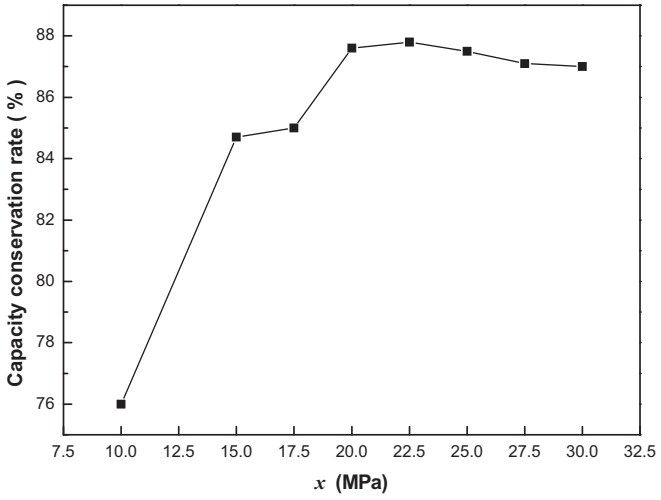

Fig. 3. The relationship between the capacity conservation rate after 100 cycles of the electrode and compaction pressure.

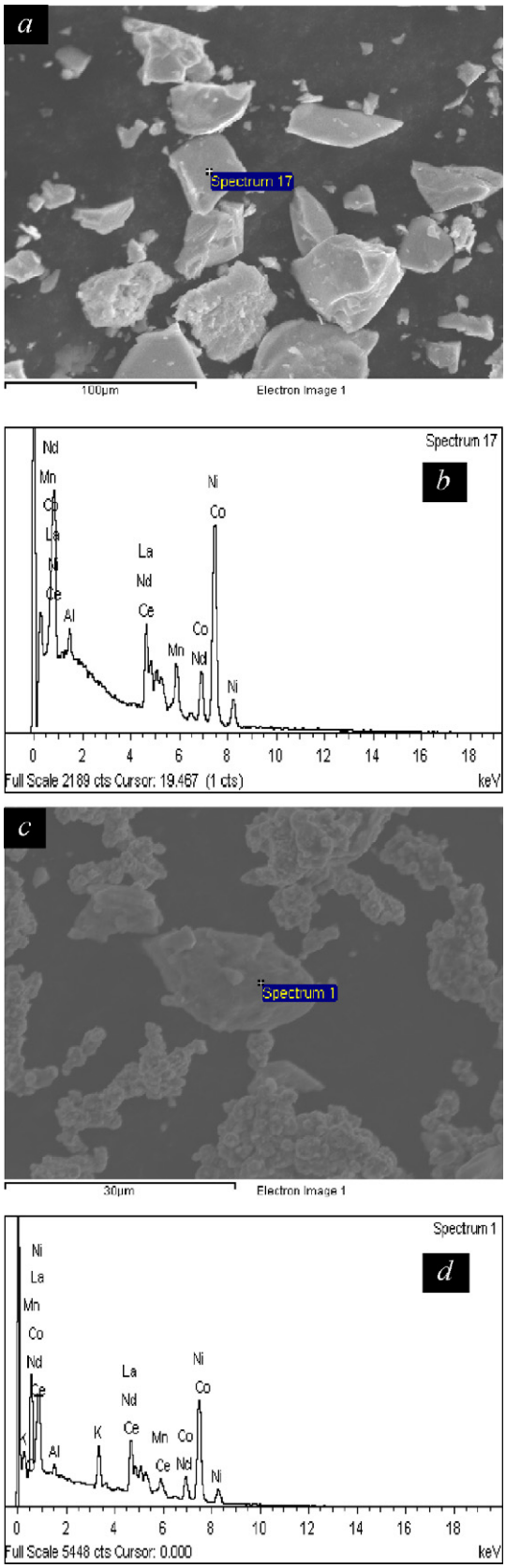

Fig. 4. SEM images and EDS patterns of the electrode alloys before and after cycles: (a and b) before cycle; (c and d) after100 cycles, alloy electrode prepared at 15 MPa.

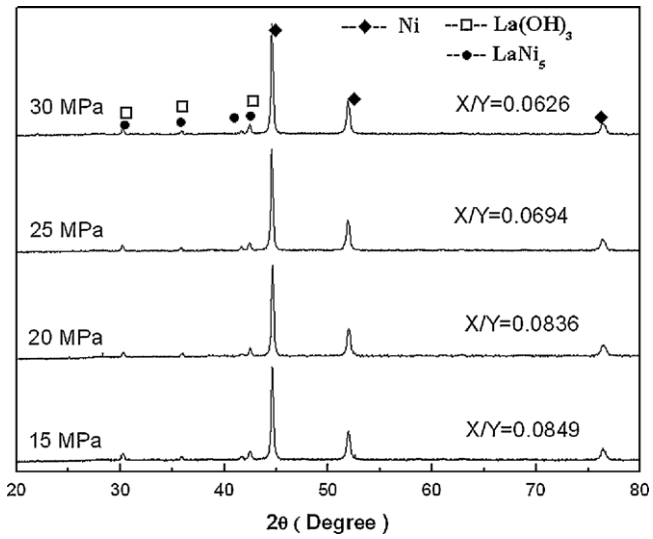

Fig. 5. XRD patterns of the electrode alloys after 100 cycles. *X* and *Y* are the integrated intensity of $La(OH)_3$ and Ni, respectively.

at 10 MPa. As the compaction pressure increases, the alloy particles closely contact with the conductive materials during electrode preparation process. The charge-transfer reaction rate at the surface of the alloy particles is accelerated and the electrochemical reactions are greatly promoted. These all result in significant improvements in the maximum discharge capacity of the electrodes.

As for the decrease of the maximum discharge capacity of the electrode prepared at over 25 MPa, it is possible that the porosity of the electrode decreases at elevated compaction pressure so that many empty spaces in the alloy particles reduce or even disappear, and the electrolyte is very difficult to enter into the surfaces of alloy particles inside the electrodes. In order to illuminate the relationship between the porosity of the electrode and compaction pressure, the densities of the electrodes prepared at different compaction pressures are measured. The results are shown in Fig. 2. It can be seen that the density of the electrode markedly increases with the increase of the compaction pressure. The smaller the density of the electrode is, the more the porosity of the electrode is. Thus, the porosity of the electrode decreases with the increase of the compaction pressure. This effectively confirms that the decrease of the maximum discharge capacity of the electrode prepared at over 25 MPa is ascribed to the decrease of the porosity in the electrode.

The cycle stability is characterized by the capacity conservation rate (S_n). The S_n is calculated by the following equation:

$$S_n(\%) = \frac{C_n}{C_{\max}} \times 100$$

where C_n is the discharge capacity after n charge/discharge cycles with the cut-off potential of −0.600 V vs. the Hg/HgO reference electrode. Fig. 3 shows the relationship between the capacity conservation rate after 100 charging/discharging cycles (S_{100} of the alloy electrode and the compaction pressure. It can be found that the alloy electrodes, which were prepared with moderately high pressures (20, 22.5 or 25 MPa), exhibited the better cycle stabilities. However, the cycle stability of the electrode prepared at the lower (10 MPa) or higher pressure (30 MPa) becomes worse.

The decrease of the cycle stability of the electrode is mainly due to a decay of the discharge capacity. Literature [26] reported that the fundamental reasons for the discharge capacity decay of the electrode are the pulverization and the corrosion of the electrode alloy during charging/discharging cycle. The lattice internal stress

Table 1
The corresponding data of EDS patterns before and after 100 charging/discharging cycles (x = 15 MPa).

Conditions	Elements								
	Al	Mn	Co	Ni	La	Ce	Nd	K	O
Before cycle									
Weight (%)	2.95	7.01	9.75	45.05	20.22	11.76	3.26		
Atomic (%)	7.68	8.98	11.64	53.97	10.24	5.91	1.59		
After cycle									
Weight (%)	1.25	3.30	6.71	34.40	19.54	11.29	2.61	3.74	17.16
Atomic (%)	2.09	2.71	5.14	26.47	6.36	3.64	0.82	4.32	48.45

and cell volume expansion, which are inevitable when hydrogen atoms enter into the interstitials of the lattice, are the real driving force that leads to the pulverization of the alloy [27]. In order to correctly explain the mechanism of the efficacy loss of the electrode, the morphologies of the electrode alloy particles before and after cycling are studied by SEM. The SEM images and EDS patterns of the alloy before and after 100 charging/discharging cycles (x = 15 MPa) are shown in Fig. 4 and the corresponding data of EDS patterns are listed in Table 1. As shown in Fig. 4, the surfaces of the alloy particles before cycling with sharp edges are bright and smooth (Fig. 4a). However, the surface morphologies of the alloys show changes after cycling, leading to a disappearance of the angular edges of the alloy particles. This confirms that the angular edges of the surfaces of the alloy particles have reacted prior to the other zones. Moreover, the surface of the alloy particles after cycling was covered with a dark, rough and porous layer (Fig. 4c). A rough and porous layer is formed due to the corrosion and the oxidation of the alloy particles in the alkaline electrolyte. Especially, it is inertial chemically so that the electrochemical reaction on the surfaces of the alloy particles is inhibited to certain extent. As a result, the capacity of the electrode decreases. Moreover, the data in Table 1 indicates that the oxide has formed after cycling. As shown in Table 1, oxygen and potassium elements exist in the electrode alloys after cycling when compared with before cycling. Oxygen element of the electrode alloy implies the formation of the oxide. As for potassium element, it comes from KOH solution as electrolyte. The above results confirm further that the oxidation of alloy particles takes place during cycling, and the oxidation degree of the alloy electrodes after cycling varies with the pressure of electrode preparation. Fig. 5 shows the XRD patterns of the electrode alloy powders removed from these electrodes prepared at different pressure after 100 charging/discharging cycles. It is found that the hydroxides of rare earth metals have formed in the electrode alloys after cycling; however, the peak intensity of the hydroxides of rare earth metals from the electrodes prepared at different pressures is varied. The amount of hydroxides of rare earth metals of the alloy electrode decreases with the increase of x. It indicates that the alloy particles are easier to be oxidized at the smaller electrode preparation pressures. This result implies that the severe oxidation of the alloy particles results in decrease in the cycle stability of the electrode prepared at 15 MPa.

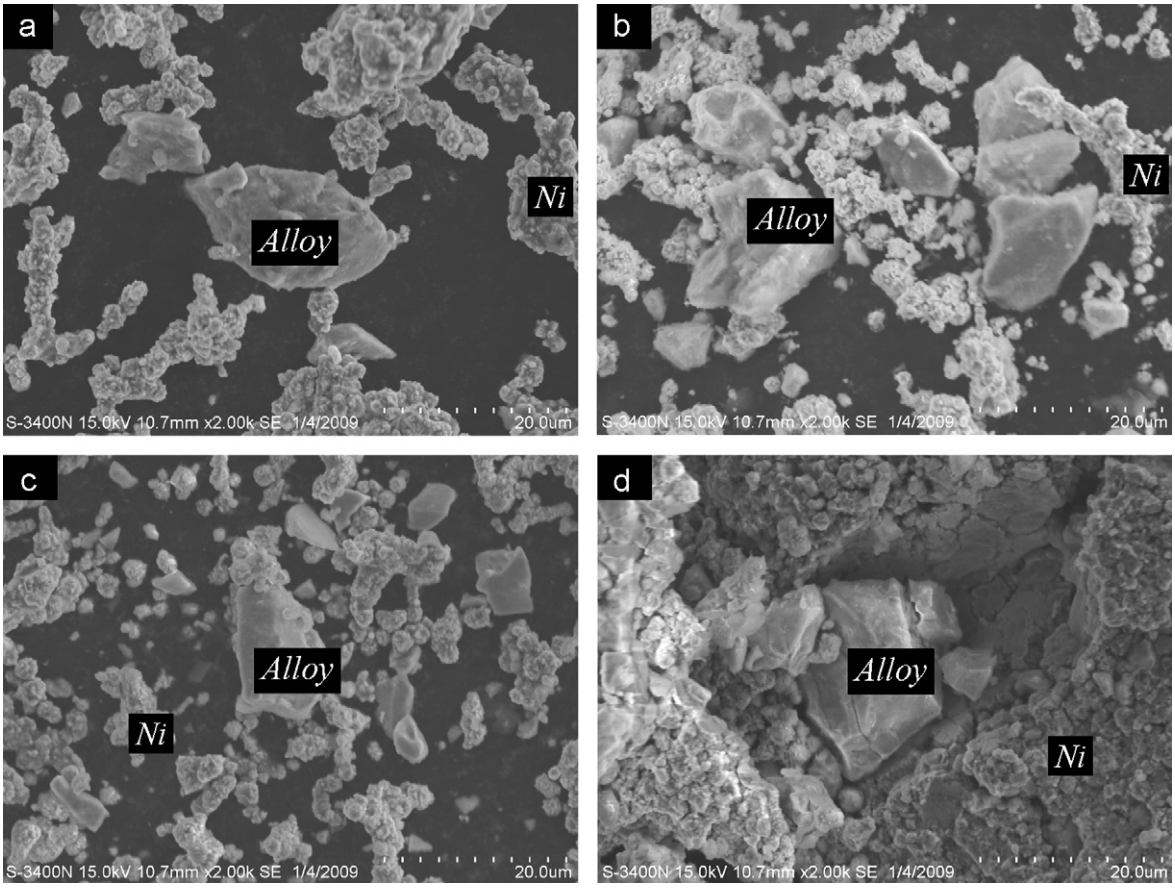

Fig. 6. The SEM images of the electrode alloys after 100 cycles: (a) 15 MPa; (b) 20 MPa; (c) 25 MPa; (d) 30 MPa.

Table 2
Lattice parameters and cell volumes of the $LaNi_5$ phase in alloys after 100 cycles.

Conditions (MPa)	Phase	Lattice parameters		V (nm^3)
		a (nm)	c (nm)	
15	$LaNi_5$	0.50211(4)	0.39684(6)	0.08665
20	$LaNi_5$	0.50139(1)	0.39889(5)	0.08684
25	$LaNi_5$	0.50099(8)	0.39884(1)	0.08666
30	$LaNi_5$	0.49793(6)	0.40556(8)	0.08711

Table 2 shows lattice parameters and cell volumes of the $LaNi_5$ phase in alloys after 100 charging/discharging cycles. It can be seen that of the $LaNi_5$ phase in the electrode alloy prepared at 30 MPa after 100 charging/discharging cycles results in the largest cell volume. The cell volume is closely related to the degree of the pulverization. In general, a larger cell volume results in higher degree of pulverization. Thus, the above result confirms that the pulverization of the electrode alloy prepared at 30 MPa is more serious than the others. Therefore, two main reasons are responsible for the poor cycle stability of the electrode prepared at 30 MPa. The first one is that the pulverization of the alloy in process of the hydrogen absorption/desorption, and the other one is that the porosity of the electrode is destroyed at high pressure and hydrogen atoms irreversibly release from the crystal lattice of $LaNi_5$.

The surface morphologies of the electrode alloys after 100 charging/discharging cycles have been investigated by SEM as shown in Fig. 6. It is obvious that the darker colour of the alloy particle surfaces is due to the corrosion and the oxidation of the alloy particles in the alkaline electrolyte. In all cases, the alloy particles of the electrode prepared at 15 MPa are corroded and oxidized to a large extent. Moreover, many fractures have been observed in the alloy particles of the electrode prepared at 30 MPa. It also reinforces the fact that the pulverization of the electrode alloy prepared at 30 MPa is more serious than the others.

4. Conclusions

In this paper, the effects of compaction pressure on the maximum discharge capacity and cycle stability of the metal hydride electrodes were investigated. Electrochemical studies show that the maximum discharge capacity of the electrode firstly increases and then decreases with the increase of compaction pressure. The electrode prepared at 25 MPa exhibits the maximum discharge capacity (368 mAh/g) higher than the others. The electrode prepared at moderately high pressures (20 or 25 MPa) exhibits better cycle stability, whereas the cycle stability of the electrode prepared at the lower (10 MPa) or higher pressure (30 MPa) becomes even worse. Taking both of discharge capacity and cycle stability of an electrode into consideration, a suitable compaction pressure for metal hydride electrodes in a Ni–MH battery should be controlled in the range of 20 to 25 MPa.

Acknowledgements

This work was supported by Foundation for Chunhui Programme of the Ministry of Education of China (No.Z2006-1-01002), The Key Industrial Technology Research and Development Programme of Guangdong province (Project No. 2007B010600030) and the Talents Development Foundation of Inner Mongolia Autonomous Region (No. 200606). We thank the editor, Dr. Hongge Pan, and two anonymous referees for detailed and thoughtful comments that helped improve the manuscript. Moreover, we also thank Dr. Zhiqiang Ou for generous help of this work.

References

[1] M.A. Fetcenko, S.R. Ovshinsky, B. Reichman, K. Young, C. Fierro, J. Koch, A. Zallen, W. Mays, T. Ouchi, J. Power Sources 165 (2007) 544–551.
[2] Peter Bäuerlein, Christina Antonius, Jens Löffler, Jörg Kümpers, J. Power Sources 176 (2008) 547–554.
[3] X.Y. Zhao, L.Q. Ma, Int. J. Hydrogen Energy 34 (2009) 4788–4796.
[4] S. Nathira Begum, V.S. Muralidharan, C. Ahmed Basha, J. Alloys Compd. 467 (2009) 124–129.
[5] X.D. Wei, H. Dong, Y.N. Liu, P. Zhang, J.W. Zhu, G. Yu, J. Alloys Compd. 481 (2009) 687–691.
[6] M. Tliha, S. Boussami, H. Mathlouthi, J. Lamloumi, A. Percheron-Guégan, J. Alloys Compd. 506 (2010) 559–564.
[7] X. Tian, X.D. Liu, J. Xu, H.W. Feng, B. Chi, L.H. Huang, S.F. Yan, Int. J. Hydrogen Energy 34 (2009) 2295–2302.
[8] K. Young, J. Koch, T. Ouchi, A. Banik, M.A. Fetcenko, J. Alloys Compd. 496 (2010) 669–677.
[9] M.X. Gao, S.C. Zhang, H. Miao, Y.F. Liu, H.G. Pan, J. Alloys Compd. 489 (2010) 552–557.
[10] M.X. Gao, H. Miao, Y. Zhao, Y.F. Liu, H.G. Pan, J. Alloys Compd. 484 (2009) 249–255.
[11] K. Young, T. Ouchi, B. Huang, B. Chao, M.A. Fetcenko, L.A. Bendersky, K. Wang, C. Chiu, J. Alloys Compd. 506 (2010) 841–848.
[12] Y.H. Zhang, D.L. Zhao, B.W. Li, H.P. Ren, S.H. Guo, X.L. Wang, J. Alloys Compd. 491 (2010) 589–594.
[13] Mustafa Anik, J. Alloys Compd. 491 (2010) 565–570.
[14] X.D. Liu, L.H. Huang, X. Tian, H.W. Feng, B. Chi, Int. J. Hydrogen Energy 32 (2007) 4939–4942.
[15] Y.H. Zhang, S.H. Guo, Y. Qi, X. Li, Z.H. Ma, Y. Zhang, J. Alloys Compd. 506 (2010) 749–756.
[16] Y. Zhao, M.X. Gao, Y.F. Liu, L. Huang, H.G. Pan, J. Alloys Compd. 496 (2010) 454–461.
[17] X.J. Zhao, Q. Li, Kuochih Chou, H. Liu, LinF G.W., J. Alloys Compd. 473 (2009) 428–432.
[18] G.Y. Shang, S.M. Han, J.S. Hao, Y. Liu, X.L. Zhu, Y. Li, D.Y. Xie, J. Alloys Compd. 493 (2010) 573–576.
[19] Z.L. Zhou, Y.Q. Song, S. Cui, C.G. Huang, W.L. Qian, C.G. Lin, Y.J. Zhang, Y.L. Lin, J. Alloys Compd. 501 (2010) 47–53.
[20] X.Y. Zhao, L.Q. Ma, Y. Ding, X.D. Shen, Int. J. Hydrogen Energy 34 (2009) 3389–3394.
[21] A.B. Yuan, N.X. Xu, J. Alloys Compd. 322 (2001) 269–275.
[22] H.W. Feng, X.D. Liu, X. Tian, B. Chi, L.H. Huang, J. Xu, Int. J. Hydrogen Energy 34 (2009) 1886–1889.
[23] X. Tian, X.D. Liu, H.W. Feng, J. Xu, J. Alloys Compd. 484 (2009) 882–885.
[24] J.E. Thomas, B.E. Castro, S. Real, A. Visintin, Int. J. Hydrogen Energy 33 (2008) 3475–3479.
[25] J.E. Thomas, E.B. Castro, A. Visintin, Int. J. Hydrogen Energy 35 (2010) 5981–5984.
[26] Daniel Chartouni, Felix Meli, Andreas Züttel, Karl Gross, Louis Schlapbach, J. Alloys Compd. 241 (1996) 160–166.
[27] Yang-Huan Zhang, Bao-Wei Li, J. Alloys Compd. 458 (2008) 340–345.